

Supplementary Information

Carbon–sulfur bond cleavage reactions of dibenzothiophene derivatives mediated by iron and ruthenium carbonyls

Masakazu Hirotsu,* Chiaki Tsuboi, Takanori Nishioka and Isamu Kinoshita

Department of Material Science, Graduate School of Science, Osaka City University, Sumiyoshi-ku, Osaka 558-8585, Japan. Fax: 816 6690 2753; Tel: 816 6605 2546; E-mail: mhiro@sci.osaka-cu.ac.jp

Experimental

General Procedures. All manipulations were performed using a glove box under an atmosphere of oxygen-free dry argon or standard Schlenk techniques under argon. Dried solvents and $[\text{Pd}(\text{PPh}_3)_4]$ were purchased from Nacalai Tesque, Inc. Dibenzothiophene was purchased from Tokyo Chemical Industry Co., Ltd. Dodecacarbonyltriruthenium and pentacarbonyliron was purchased from Aldrich Chemical Co. and Kanto Chemical Co., Inc., respectively. The compounds dibenzothiophene-4-boronic acid,¹ 4-(2'-pyridyl)dibenzothiophene (PyDBT),² and 6-bromo-2,2'-bipyridine,³ and $C_r[\text{Ru}(\mu\text{-PyBPT}-\kappa^3N,C,S)(\text{CO})_2]_2$ (**1a**)² were prepared according to literature procedures. NMR spectra were recorded on a JEOL Lambda 300, a JEOL Lambda 400, or a Bruker AVANCE 300 FT-NMR spectrometer at room temperature. IR spectra were obtained on a JASCO FT/IR-6200 spectrometer at room temperature. ESI mass spectrometry was performed on an Applied Biosystem Mariner time-of-flight mass spectrometer. Elemental analyses were performed by the Analytical Research Service Center at Osaka City University on J-SCIENCE LAB JM10 or FISONS Instrument EA1108 elemental analyzers. Photolysis was carried out using an Ushio UM-452 450W high-pressure Hg lamp placed in a water-cooled quartz jacket.

Synthesis of 6-(4''-dibenzothienyl)-2,2'-bipyridine (bpyDBT). A solution of K_2CO_3 in 1,2-dimethoxyethane/ H_2O (3:1, 20 mL) was deoxygenated by bubbling with argon gas. Dibenzothiophene-4-boronic acid (0.46 g, 2.0 mmol), 6-bromo-2,2'-bipyridine (0.47 g, 2.0 mmol), and $[\text{Pd}(\text{PPh}_3)_4]$ (23 mg, 0.020 mmol) were added, and then the mixture was stirred at 100 °C for 6 h. To the resulting yellow

solution was added water (50 mL), and the mixture was extracted with chloroform (80 mL). The extract was dried over anhydrous Na_2SO_4 , filtered, and concentrated to dryness. The residual pale brown oil was purified by column chromatography (silica gel, 2 cm \times 18 cm, *n*-hexane/ethyl acetate, 1:1) to afford an off-white solid. Recrystallization from dichloromethane-methanol gave pure bpyDBT as colorless crystals (0.49 g, 72%). ^1H NMR (300 MHz, CDCl_3): δ 7.38 (ddd, J = 7.5, 4.8, 1.2 Hz, 1H, 5'-bpy), 7.50 (m, 2H, 7-DBT, 8-DBT), 7.63 (t, J = 7.7 Hz, 1H, 2-DBT), 7.92–8.03 (m, 4H, 4-bpy, 5-bpy, 4'-bpy, 6- or 9-DBT), 8.07 (dd, J = 7.6, 1.0 Hz, 1H, 1- or 3-DBT), 8.19–8.26 (m, 1H, 6- or 9-DBT), 8.29 (dd, J = 7.8, 1.0 Hz, 1H, 1- or 3-DBT), 8.49 (m, 1H, 3-bpy), 8.75 (ddd, J = 4.8, 1.7, 0.9 Hz, 1H, 6'-bpy), 8.99 (ddd, J = 8.0, 1.2, 0.9 Hz, 1H, 3'-bpy). $^{13}\text{C}\{\text{H}\}$ NMR (75.5 MHz, CDCl_3): δ 120.0, 121.5, 122.3, 122.51, 122.55, 124.1, 124.2, 124.7, 125.5, 126.8, 133.4, 134.8, 137.3, 137.85, 137.94, 141.7, 148.5, 155.0, 155.6, 155.9. Anal. Calcd for $\text{C}_{22}\text{H}_{14}\text{N}_2\text{S}$: C 78.08, H 4.17, N 8.28. Found: C 78.08, H 4.13, N 8.34. The ^1H and $^{13}\text{C}\{\text{H}\}$ NMR spectra are shown in Figs. S1 and S2, respectively.

Synthesis of 2. A Pyrex sample tube with a Teflon valve was charged with bpyDBT (34 mg, 0.10 mmol), $[\text{Ru}_3(\text{CO})_{12}]$ (64 mg, 0.10 mmol), and toluene (1.5 mL). The tube was sealed, and then the orange suspension was stirred at 100 °C for 4 h to give a dark brown suspension. The toluene solution was decanted, and the residue was extracted by decantation with ethyl acetate (2 mL \times 5). The collected bright yellow solution was purified by column chromatography (silica gel, *n*-hexane/ethyl acetate, 1:1). The first yellow band contained $[\text{Ru}_3(\text{CO})_{12}]$. The second yellow band was collected, and the solvent was removed to afford a yellow powder of **2** (15 mg, 17%). ^1H NMR (300 MHz, CD_2Cl_2): δ 6.95 (dd, J = 7.4, 1.2 Hz, 1H), 7.16 (t, J = 7.6 Hz, 1H), 7.30–7.35 (m, 1H), 7.47–7.58 (m, 3H), 7.71–7.75 (m, 1H), 7.79 (dd, J = 7.8, 1.2 Hz, 1H), 7.93 (dd, J = 7.3, 1.1 Hz, 1H), 8.00–8.12 (m, 3H), 8.21 (d, J = 8.0 Hz, 1H), 8.69 (d, J = 5.0 Hz, 1H). $^{13}\text{C}\{\text{H}\}$ NMR (75.5 MHz, CD_2Cl_2): δ 119.0, 120.6, 123.8, 123.9, 124.2, 127.3, 127.5, 128.8, 130.9, 131.4, 132.6, 139.0, 144.5, 145.5, 149.5, 152.9, 153.7, 154.0, 157.0, 164.8, 167.2, 188.0, 195.4, 199.6, 199.9, 200.5. Anal. Calcd for $\text{C}_{31}\text{H}_{14}\text{N}_2\text{O}_9\text{Ru}_3\text{S}$: C, 41.66; H, 1.58; N, 3.13. Found: C, 41.74; H, 1.49; N, 3.09. IR (KRS): $\nu_{\text{CO}}/\text{cm}^{-1}$ 2066, 2028, 2021, 1989, 1982, 1958, 1949. The ^1H and $^{13}\text{C}\{\text{H}\}$ NMR spectra are shown in Figs. S3 and S4, respectively. Crystals suitable for X-ray structure analysis were grown from an acetone solution of **2**.

Synthesis of $[\{\text{Fe}(\mu\text{-PyBPT-}\kappa^3\text{N,C,S})(\text{CO})_2\}\text{Fe}(\text{CO})_3]$ (3). A quartz glass sample tube with a Teflon valve was charged with PyDBT (97 mg, 0.37 mmol), $[\text{Fe}(\text{CO})_5]$ (100

μL , 0.74 mmol), and THF (25 mL). The yellow solution was degassed three times using a freeze-pump-thaw method, and then the tube was sealed. The solution was irradiated with a high-pressure Hg lamp for 9 h, during which time the reaction solution was degassed every 3 h. The color of the solution changed to purple. The solvent was removed to leave a purple solid, which was purified by column chromatography (silica gel, *n*-hexane/dichloromethane, 2:1). A purple band was collected and concentrated, and then *n*-hexane was added. Dark purple crystals of **3** were collected by filtration and washed with *n*-hexane (82 mg, 43%). ^1H NMR (300 MHz, CDCl_3): δ 6.79 (ddd, $J = 7.7, 5.8, 2.7$ Hz, 1H, 3, 4 or 5-BPT), 6.98-7.08 (m, 3H, 6-BPT, 3, 4 or 5-BPT), 7.14 (ddd, $J = 7.3, 5.6, 1.5$ Hz, 1H, 5-py), 7.28 (dd, $J = 8.4, 7.1$ Hz, 1H, 5'-BPT), 7.47 (dd, $J = 7.1, 0.6$ Hz, 1H, 4'-BPT), 7.69 (m, 1H, 4-py), 7.77 (m, 1H, 3-py), 8.26 (dd, $J = 8.4, 0.6$ Hz, 1H, 6'-BPT), 9.22 (d, br, $J = 5.6$ Hz, 1H, 6-py). $^{13}\text{C}\{^1\text{H}\}$ NMR (100 MHz, CDCl_3): δ 119.15, 119.22, 122.9, 124.1, 125.6, 126.6, 127.9, 129.1, 129.4, 133.4, 136.2, 138.7, 144.8, 155.2, 157.5, 163.4, 167.9, 212.2, 213.5, 213.6. Anal. Calcd for $\text{C}_{22}\text{H}_{11}\text{Fe}_2\text{NO}_5\text{S}$: C, 51.50; H, 2.16; N, 2.73. Found: C, 51.66; H, 2.18; N, 2.66. IR (KRS): $\nu_{\text{CO}/\text{cm}^{-1}} = 2030, 1965, 1934, 1920$. UV-Vis: $\lambda_{\text{max}}(\text{CH}_2\text{Cl}_2)/\text{nm}$ 524 ($\epsilon/\text{dm}^3 \text{ mol}^{-1} \text{ cm}^{-1}$ 3400). The ^1H and $^{13}\text{C}\{^1\text{H}\}$ NMR spectra are shown in Figs. S5 and S6, respectively. The absorption spectrum is shown in Fig. S10. Crystals suitable for X-ray structure analysis were grown by diffusion of cyclohexane into a toluene solution of **3**.

Synthesis of $[\{\text{Fe}(\mu\text{-bpyBPT-}\kappa^3\text{N,C,S})(\text{CO})_2\}\text{Fe}(\text{CO})_3]$ (4). A Pyrex sample tube with a Teflon valve was charged with bpyDBT (34 mg, 0.10 mmol), $[\text{Fe}(\text{CO})_5]$ (27 μL , 0.20 mmol), and THF (1.5 mL). The yellow solution was degassed three times using a freeze-pump-thaw method, and then the tube was sealed. The solution was irradiated with a high-pressure Hg lamp for 10 h to give a purple suspension. The solvent was removed under reduced pressure. The purple residue was washed with a mixture of toluene and *n*-hexane (1:1, 1 mL), and then washed with *n*-hexane (1 mL \times 3). The resulting purple solid was dissolved in a minimal amount of dichloromethane and filtered through Celite. The purple filtrate was layered with *n*-hexane. After two weeks, purple microcrystals of **4** were collected by filtration and washed with *n*-hexane (14 mg, 25%). ^1H NMR (400 MHz, CDCl_3): δ 6.73-6.81 (m, 1H, 4 or 5-BPT), 6.95-7.01 (m, 2H, 4 or 5-BPT, 6-BPT), 7.11-7.18 (m, 2H, 3-BPT, 5'-BPT), 7.40-7.45 (m, 2H, 4'- or 5'-bpy, 4'-BPT), 7.65 (dd, $J = 7.8, 0.7$ Hz, 1H, 5-bpy), 7.75 (t, $J = 7.8$ Hz, 1H, 4-bpy), 7.92 (td, $J = 7.8, 1.4$ Hz, 1H, 4'- or 5'-bpy), 7.92 (dd, $J = 7.8, 0.7$ Hz, 1H, 3-bpy), 8.05 (dd, $J = 8.4, 0.8$ Hz, 1H, 6'-BPT), 8.22 (d, br, $J = 7.9$ Hz, 1H, 3'-bpy), 9.01 (d, br, $J = 5.6$ Hz, 1H, 6'-bpy). $^{13}\text{C}\{^1\text{H}\}$ NMR (100 MHz, CDCl_3): δ 116.5, 117.9, 120.8, 122.2,

124.5, 124.6, 125.9, 126.8, 128.7, 128.9, 129.0, 133.3, 134.8, 136.0, 136.9, 145.2, 153.0, 155.3, 157.6, 157.7, 161.3, 162.3, 209.7, 217.4. Anal. Calcd for C₂₆H₁₄Fe₂N₂O₄S: C, 55.55; H, 2.51; N, 4.98. Found: C, 55.31; H, 2.51; N, 4.89. IR (KRS): $\nu_{\text{CO}}/\text{cm}^{-1}$ 1991, 1936, 1891. UV-Vis: $\lambda_{\text{max}}(\text{CH}_2\text{Cl}_2)/\text{nm}$ 544 ($\epsilon/\text{dm}^3 \text{ mol}^{-1} \text{ cm}^{-1}$ 5800). The ¹H and ¹³C{¹H} NMR spectra are shown in Figs. S7 and S8, respectively. The absorption spectrum is shown in Fig. S10.

NMR experiments for the reaction of [Ru₃(CO)₁₂] with bpyDBT. An NMR tube with a Teflon valve was charged with bpyDBT (10 mg, 0.030 mmol), [Ru₃(CO)₁₂] (19 mg, 0.030 mmol), mesitylene (2.8 μL , 0.020 mmol) as an internal standard, and toluene-*d*₈ (0.5 mL). The tube was heated at 100 °C, and ¹H NMR measurements were performed. The time course of the conversion of bpyDBT to **2** is shown in Fig. S9.

Thermal reaction of *C*_r-[Ru(μ -PyBPT- κ^3 N,C,S)(CO)₂]₂ (1a**).** An NMR tube with a Teflon valve was charged with **1a** and toluene-*d*₈. The tube was heated at 100 °C for 27 h, and ¹H NMR measurements were performed. No change was observed in the NMR spectra as shown in Fig. S11.

Photolysis of [Fe(CO)₅] and dibenzothiophene. A Pyrex sample tube with a Teflon valve was charged with dibenzothiophene (27 mg, 0.15 mmol), [Fe(CO)₅] (40 μL , 0.30 mmol), and THF (10 mL). The yellow solution was degassed three times using a freeze-pump-thaw method, and then the tube was sealed. The solution was irradiated with a high-pressure Hg lamp for 3 h, and then degassed. The irradiation was carried out for additional 2 h to give a pale orange-red solution. The volatile was removed under reduced pressure, and the ¹H NMR spectrum of the residue was measured in C₆D₆ (Fig. S12).

Computational details. Structure optimization and time-dependent DFT (TD-DFT) calculations of complex **3** were performed using the Gaussian 03 program package.⁴ The B3LYP density functional method and the 6-31G(d) basis set were used for the calculations. The initial model for **3** was obtained from the crystal structure determined in this work. The optimized structure of **3** is shown in Fig. S13, and its molecular coordinates are listed in Table S1. Calculated electronic transitions are presented in Table S2. The ground state molecular orbitals are illustrated in Fig. S14. The HOMO has an Fe–Fe bonding character with d(metal)- π (ligand) interactions. The HOMO-1 or HOMO-2 is a mixture of ligand π and metal d π orbitals. Although the LUMO, LUMO+1, or LUMO+2 is composed of ligand π^* and metal d orbitals, the π^*

system of the PyBPT ligand largely contributes to the molecular orbitals. Therefore the transitions from HOMO to LUMO, LUMO+1, and LUMO+2 are assignable to metal-metal-to-ligand charge transfer (MMLCT). Transitions to three excited states presented in Table S2 are calculated to be 542.15 ($f = 0.0128$), 523.84 ($f = 0.0134$), and 516.22 nm ($f = 0.0555$), and each transition has the MMLCT character. Thus the lowest absorption band for **3** (524 nm, $\epsilon = 3400 \text{ dm}^3 \text{ mol}^{-1} \text{ cm}^{-1}$) is assignable to MMLCT transitions.

References

- 1 H. J. Reich, B. Ö. Gudmundsson, D. P. Green, M. J. Bevan and I. L. Reich, *Helv. Chim. Acta* 2002, **85**, 3748–3772.
- 2 M. Shibue, M. Hirotsu, T. Nishioka and I. Kinoshita, *Organometallics*, 2008, **27**, 4475–4483.
- 3 Y.-Q. Fang and G. S. Hanan, *Synlett*, **2003**, 852–854.
- 4 Gaussian 03, Revision B.05, M. J. Frisch, G. W. Trucks, H. B. Schlegel, G. E. Scuseria, M. A. Robb, J. R. Cheeseman, J. A. Montgomery, Jr., T. Vreven, K. N. Kudin, J. C. Burant, J. M. Millam, S. S. Iyengar, J. Tomasi, V. Barone, B. Mennucci, M. Cossi, G. Scalmani, N. Rega, G. A. Petersson, H. Nakatsuji, M. Hada, M. Ehara, K. Toyota, R. Fukuda, J. Hasegawa, M. Ishida, T. Nakajima, Y. Honda, O. Kitao, H. Nakai, M. Klene, X. Li, J. E. Knox, H. P. Hratchian, J. B. Cross, C. Adamo, J. Jaramillo, R. Gomperts, R. E. Stratmann, O. Yazyev, A. J. Austin, R. Cammi, C. Pomelli, J. W. Ochterski, P. Y. Ayala, K. Morokuma, G. A. Voth, P. Salvador, J. J. Dannenberg, V. G. Zakrzewski, S. Dapprich, A. D. Daniels, M. C. Strain, O. Farkas, D. K. Malick, A. D. Rabuck, K. Raghavachari, J. B. Foresman, J. V. Ortiz, Q. Cui, A. G. Baboul, S. Clifford, J. Cioslowski, B. B. Stefanov, G. Liu, A. Liashenko, P. Piskorz, I. Komaromi, R. L. Martin, D. J. Fox, T. Keith, M. A. Al-Laham, C. Y. Peng, A. Nanayakkara, M. Challacombe, P. M. W. Gill, B. Johnson, W. Chen, M. W. Wong, C. Gonzalez, and J. A. Pople, Gaussian, Inc., Pittsburgh PA, 2003.

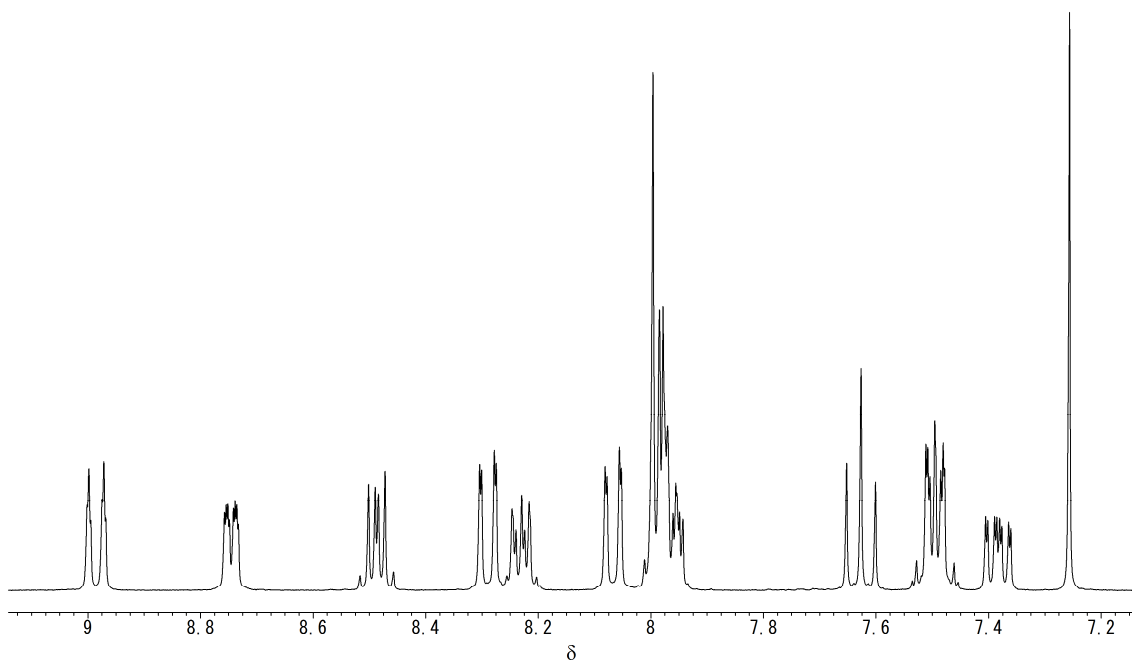


Fig. S1. ¹H NMR spectrum (300 MHz, CDCl₃) of bpyDBT.

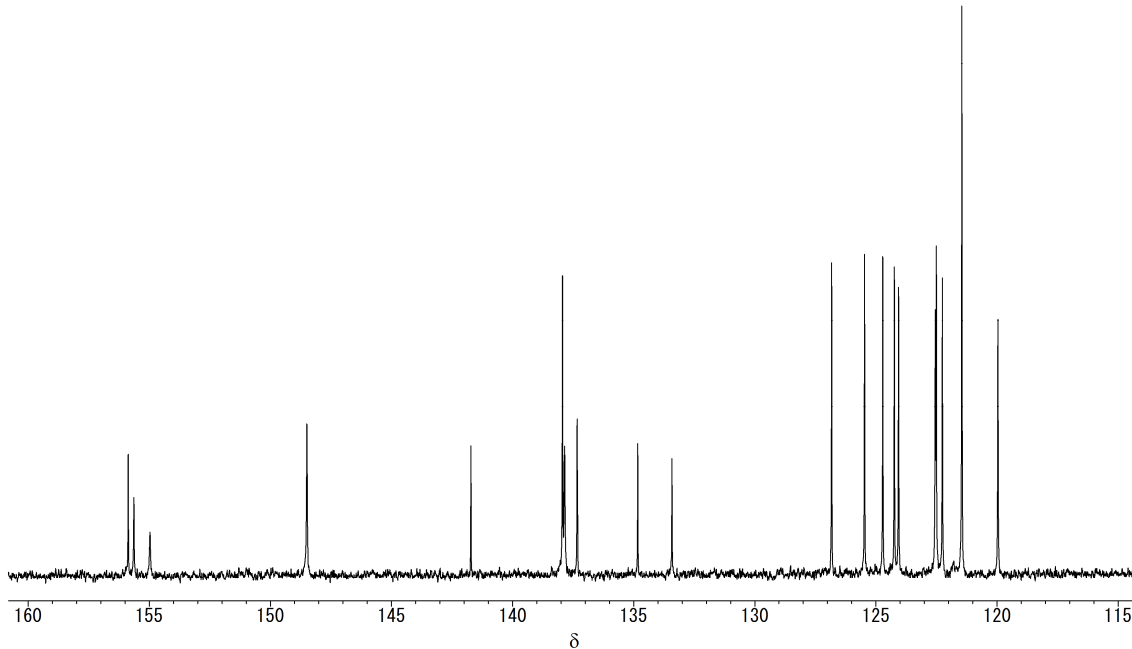


Fig. S2. ¹³C{¹H} NMR spectrum (75.5 MHz, CDCl₃) of bpyDBT.

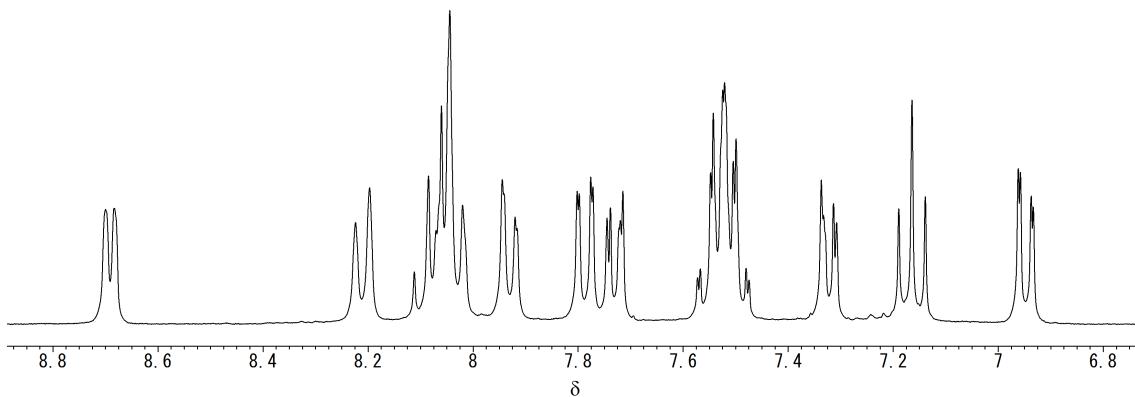


Fig. S3. ^1H NMR spectrum (300 MHz, CD_2Cl_2) of **2**.

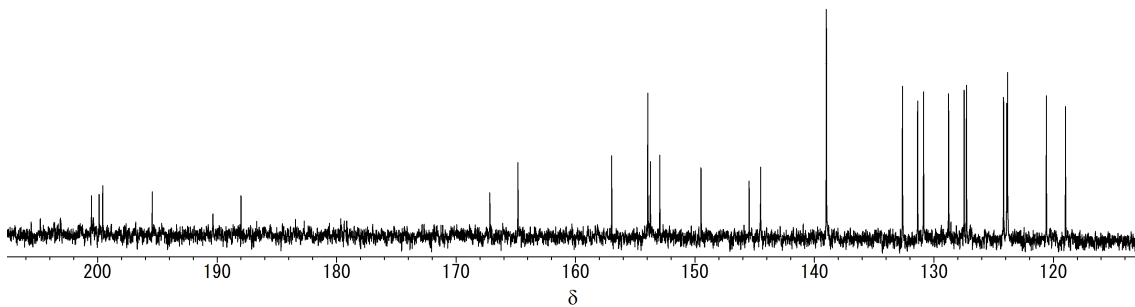


Fig. S4. $^{13}\text{C}\{^1\text{H}\}$ NMR spectrum (75.5 MHz, CD_2Cl_2) of **2**.

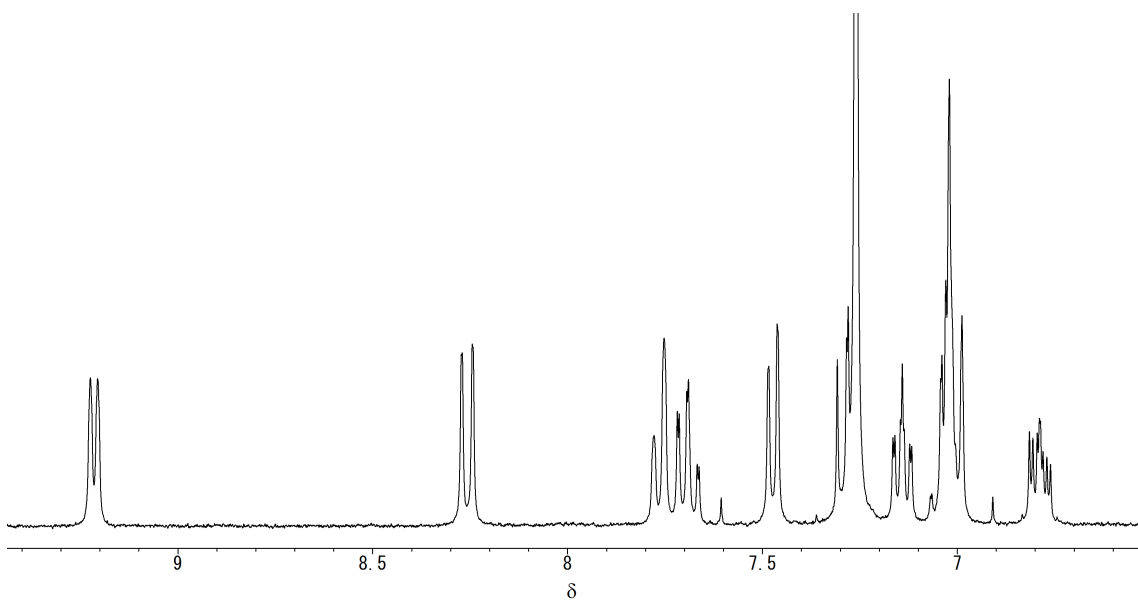


Fig. S5. ¹H NMR spectrum (300 MHz, CDCl₃) of **3**.

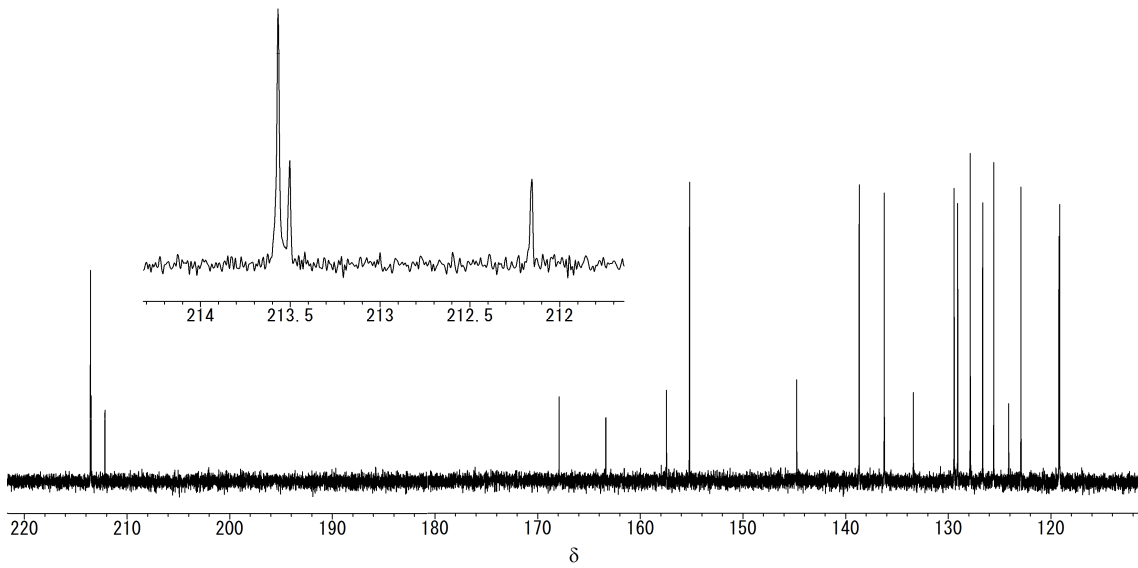


Fig. S6. ¹³C{¹H} NMR spectrum (100 MHz, CDCl₃) of **3**.

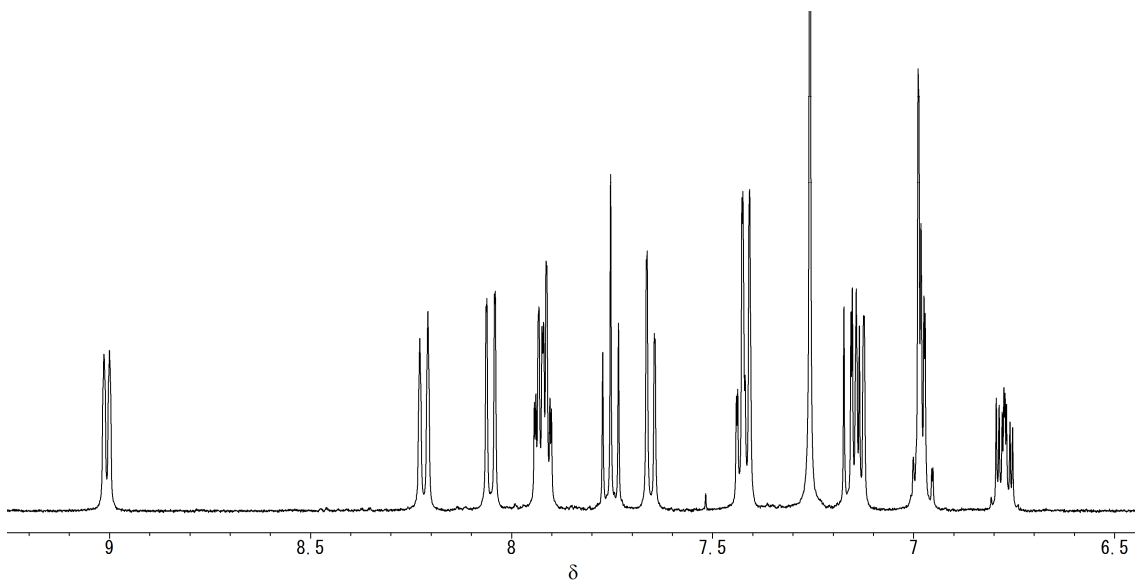


Fig. S7. ¹H NMR spectrum (400 MHz, CDCl₃) of **4**.

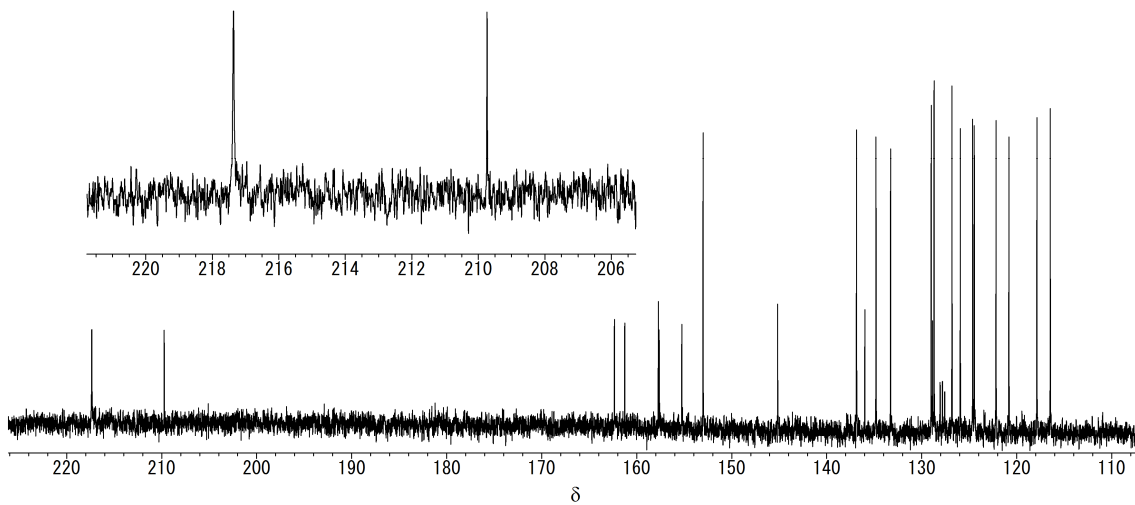


Fig. S8. ¹³C{¹H} NMR spectrum (100 MHz, CDCl₃) of **4**.

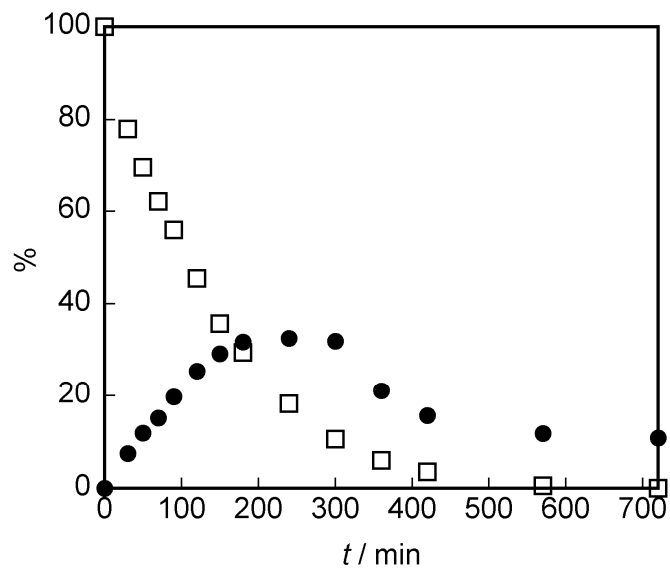


Fig. S9. Plot of conversion of bpyDBT (\square) to **2** (\bullet) as a function of time.

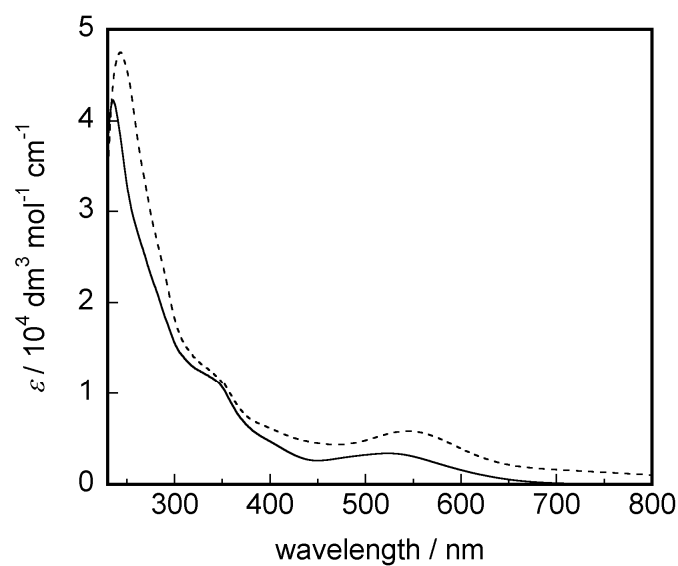


Fig. S10. Absorption spectra of **3** (—) and **4** (---) in dichloromethane.

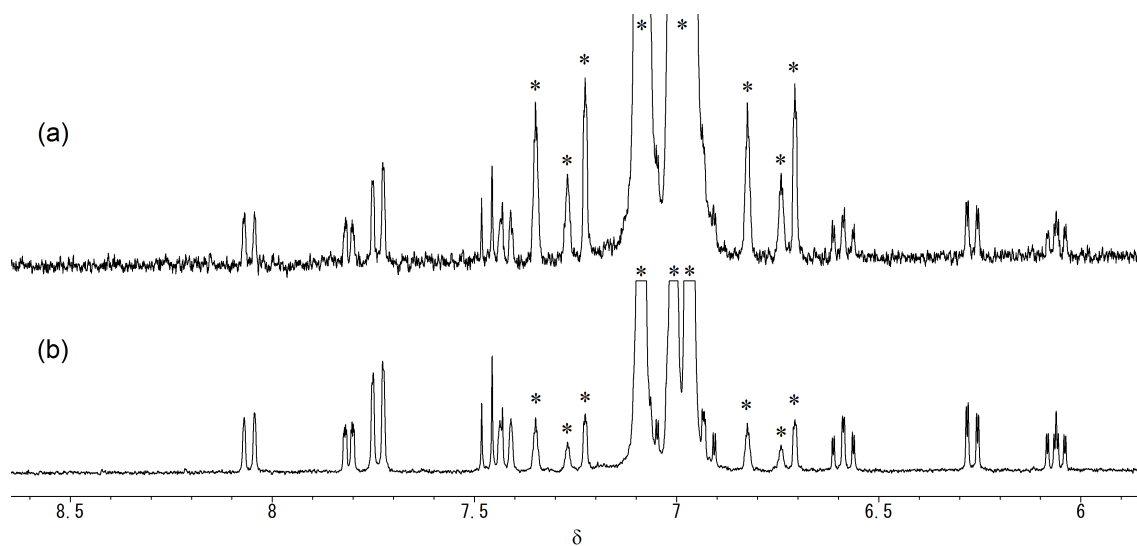


Fig. S11. ¹H NMR spectra (300 MHz) of **1a** in toluene-*d*₈ after heating at 100 °C for (a) 0 h and (b) 27 h. Residual solvent signals are marked with an asterisk.

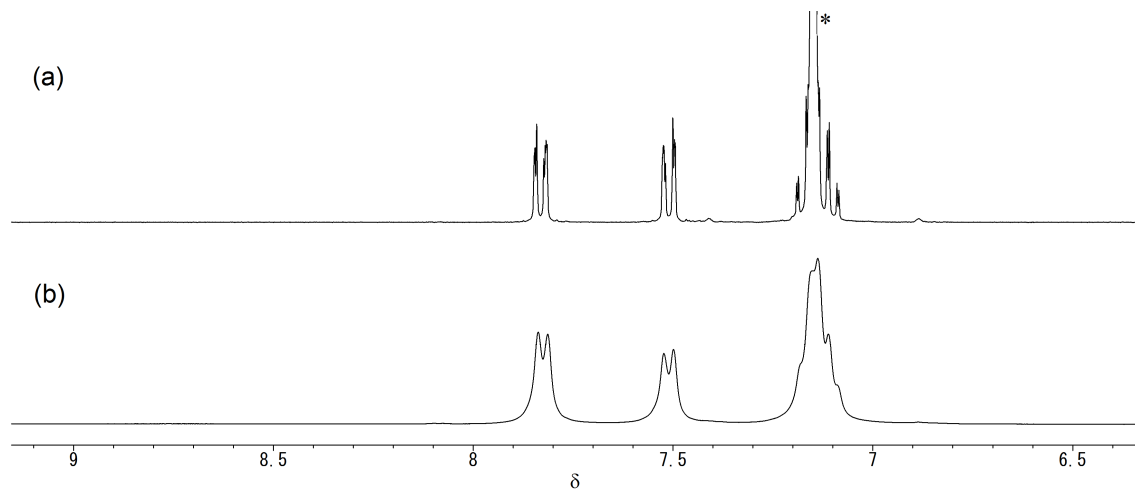


Fig. S12. ¹H NMR spectra (300 MHz, C₆D₆) of (a) dibenzothiophene and (b) the reaction products for photolysis of [Fe(CO)₅] and dibenzothiophene in THF. A residual solvent signal is marked with an asterisk.

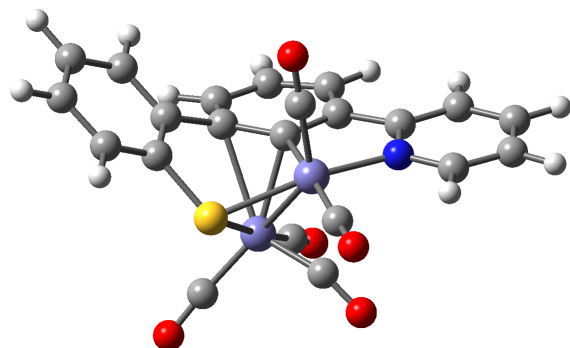


Fig. S13. Molecular structure of **3** optimized by the DFT calculation.

Table S1. Molecular coordinates of **3** optimized by the density functional calculation

	Atomic number	x/Å	y/Å	z/Å
1	26	0.359897	0.693005	1.378443
2	26	-0.560846	-1.175431	-0.035602
3	16	1.493138	-1.301630	1.011965
4	8	-1.880936	-0.454810	2.795670
5	8	2.034820	1.240487	3.702825
6	8	-1.418787	-3.706730	1.228220
7	8	-0.950278	3.291271	1.638716
8	8	0.112353	-2.367582	-2.601337
9	7	-2.379164	-0.569755	-0.598083
10	6	1.403536	1.060417	2.752520
11	6	-1.023392	-0.193632	2.044635
12	6	-0.449323	2.258522	1.526547
13	6	-1.093473	-2.700639	0.770497
14	6	2.712433	-0.815799	-0.193677
15	6	3.852112	-1.604821	-0.355015
16	6	-3.521743	-1.270327	-0.450755
17	6	-4.758636	-0.795901	-0.859925
18	6	-0.030728	0.585368	-0.743433
19	6	1.273598	1.178592	-0.843067
20	6	2.520546	0.354824	-0.946231
21	6	4.835462	-1.235939	-1.273977
22	6	-2.432868	0.669682	-1.168463

23	6	1.369981	2.547809	-1.232455
24	6	-1.139577	1.347082	-1.249866
25	6	-4.825483	0.468342	-1.450144
26	6	-0.152408	-1.917488	-1.573383
27	6	-3.657394	1.200677	-1.600456
28	6	0.268198	3.269108	-1.651283
29	6	3.510434	0.690554	-1.884599
30	6	-0.989100	2.649881	-1.710632
31	6	4.659273	-0.086109	-2.041029
32	1	-3.430857	-2.244255	0.014952
33	1	-5.643223	-1.406096	-0.714367
34	1	-5.774925	0.875340	-1.785122
35	1	-3.685258	2.185394	-2.052039
36	1	-1.839417	3.215006	-2.081023
37	1	0.376228	4.307676	-1.949125
38	1	2.346459	3.023511	-1.226631
39	1	3.368854	1.556865	-2.522691
40	1	5.407613	0.205441	-2.772635
41	1	5.726563	-1.846289	-1.390022
42	1	3.970500	-2.497446	0.252351

Table S2. Energies of electronic transitions of **3** calculated by TD-DFT

State	Component (coefficient) ^a	E/eV	λ/nm	f^b
1 (singlet-A)	H→L (-0.29711)	2.2869	542.15	0.0128
	H→L+1 (0.53786)			
	H→L+2 (0.11654)			
2 (singlet-A)	H-4→L+1 (0.10748)	2.3668	523.84	0.0134
	H-3→L+1 (0.13999)			
	H-3→L+3 (-0.11074)			
	H-2→L+1 (0.24232)			
	H-2→L+3 (-0.11877)			
	H-2→L+5 (0.11308)			
	H-1→L (0.16301)			
	H-1→L+1 (0.17281)			
	H-1→L+3 (-0.12310)			
	H→L (0.31497)			
	H→L+1 (0.23730)			
3 (singlet-A)	H-2→L (-0.12118)	2.4018	516.22	0.0555
	H-2→L+1 (-0.15742)			
	H-2→L+3 (0.12186)			
	H-1→L+1 (-0.19826)			
	H→L (0.45087)			
	H→L+1 (0.21037)			
	H→L+3 (-0.12112)			

^a H = HOMO, L = LUMO.

^b Oscillator strength.

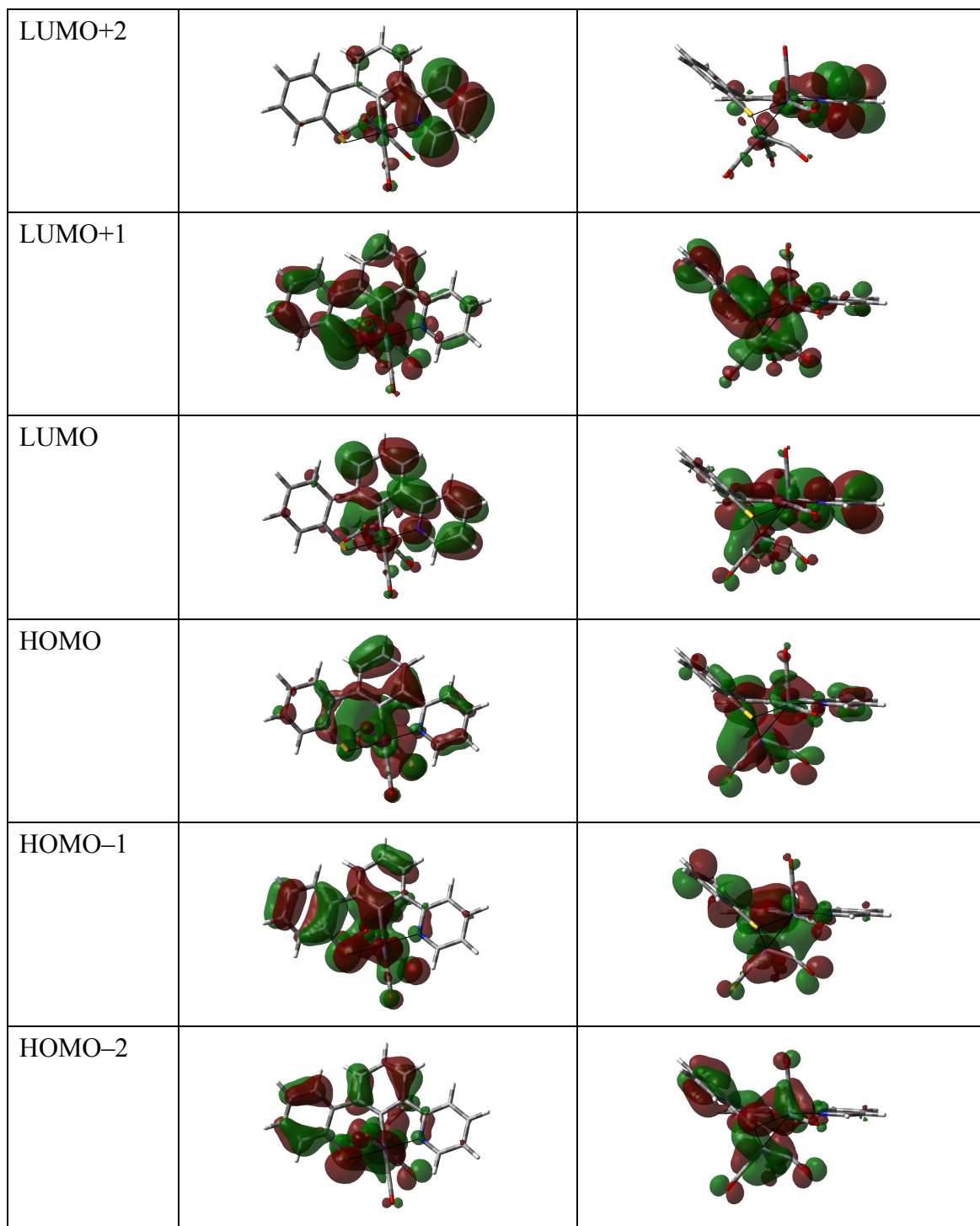


Fig. S14. Selected molecular orbitals of **3** calculated by DFT.